Conduction-band states in GaSb(110) and GaP(110) at the Brillouin-zone center

Jürgen Faul, Georg Neuhold,* and Lothar Ley
Institut für Technische Physik, Friedrich-Alexander-Universität Erlangen-Nürnberg, D-91058 Erlangen, Germany

Jordi Fraxedas
European Organization for Nuclear Research (CERN) CH-1211 Genf 23, Switzerland

Stefan Zollner
Ames Laboratory and Department of Physics and Astronomy, Iowa State University, Ames, Iowa 50011

John D. Riley and Robert C. G. Leckey
Department of Physics, La Trobe University, Bundoora, Victoria, 3083 Australia
(Received 1 June 1993; revised manuscript received 4 August 1993)

Angle-resolved constant-initial-state spectroscopy (ARCIS) from the valence-band maximum (VBM) as initial state was used to determine conduction-band energies at the Γ point up to 66 eV above the VBM for GaSb and GaP. With the help of nonlocal-empirical-pseudopotential (EPM) calculations, structure in the ARCIS spectra up to 17 eV can be assigned to particular interband transitions. The experimental results are discussed in light of our previous work on the conduction-band states of GaAs, InP, and InAs. Above 40 eV there appears to be no correspondence between conduction-band states as calculated in the EPM framework and structure in the spectra. Autoionizing resonances due to surface core excitons have been observed in both materials. From their energies a surface core-exciton binding energy of 0.6 eV for GaSb and 1.4 eV for GaP has been determined.

I. INTRODUCTION

The experimental determination of the band structure of occupied states (valence bands) of semiconductors has been performed in recent years by means of angle-resolved photoemission spectroscopy (ARPES). In most cases good agreement between band-structure calculations and the experimental data is found.[1] The interpretation of ARPES data does, however, rely on certain assumptions about the energy dispersion of the final states involved in the transitions. These assumptions are necessary to determine the wave vector $\mathbf{k}$ of the initial states because its component perpendicular to the surface $k_\perp$ is not conserved in the photoemission process. To this end the free-electron parabola (FEP) is widely used as a model dispersion for the conduction states which provides the necessary link between final-state energy and $k_\perp$. A question of importance is thus whether this model can be justified by experimental results.

In an earlier publication we have used angle-resolved constant-initial-state (ARCIS) experiments to determine the conduction-band states in GaAs, InP, and InAs (110) at Γ, the Brillouin-zone center, up to an energy of 66 eV above the valence-band maximum (VBM).[2] Here we report on an extension to GaSb and GaP (110). These measurements complement earlier $\mathbf{k}$-resolved inverse photoemission (KRIPES) investigations which yield conduction-band states up to about 5 eV above VBM.[3–5]

ARCIS is a variant of photoemission spectroscopy pioneered by Knapp and Lapeyre.[6] Here the electron energy K and the photon energy $h\nu$ are scanned in parallel such that the difference $h\nu - K = E_i$ remains fixed. Thereby it is ensured that photoemission always proceeds from initial states with the same energy E_i. By choosing the valence-band maximum as the initial state E_i the determination of conduction-band states is completely independent of any *a priori* assumption concerning the $\mathbf{k}$ vectors of initial or final states. Because for GaP and GaSb the VBM lies at $\mathbf{k}=\mathbf{0}$ (Γ point) direct transitions connect this state to final states at Γ only.

An earlier ARCIS experiment for GaP was carried out to determine the position of the surface core exciton but did not identify particular interband transitions.[7] For GaSb no ARCIS study has been reported until now.

There are several investigations of the valence-band structure of GaSb and GaP, the two materials considered in this study, by means of photoemission. The valence-band dispersion of GaP was first determined by Solal *et al.*[8] Williams *et al.*[9] studied GaSb and GaP in their extensive study of different III-V semiconductors. A recent photoemission experiment on GaSb by Manzke *et al.*[10] has led to a controversial discussion about the energetic position of the topmost occupied surface state on the (110) surface. They placed it at $\bar{\Gamma}$, the center of the surface Brillouin zone, at an energy above the VBM and thus in the bulk band gap. In a previous study of GaSb by Chiang and Eastman,[11] however, this surface state was not observed at all.

II. EXPERIMENTAL AND THEORETICAL DETAILS

The measurements were performed at the Berliner Elektronenspeicherring-Gesellschaft für Synchrotronstrahlung (BESSY) in Berlin using the TGM-4 beam line

TABLE I. Form factors (in Ry), effective-mass parameter m^*/m_0, and lattice constants a (in Å) used for the EPM calculation. Values in parentheses served as starting points for the fitting procedure.

	$V^s(3)$	$V^s(8)$	$V^s(11)$	$V^a(3)$	$V^a(4)$	$V^a(11)$ $=V^a(12)$	m^*/m_0	a
GaSb	−0.2043	0.0210	0.0558	0.0497	0.0214	0.0297	1.031	6.10
	(−0.22)	(0.00)	(0.05)	(0.06)	(0.05)	(0.01)		
GaP	−0.2281	0.0284	0.1482	0.0880	0.0529	0.0843	0.930	5.45
	(−0.22)	(0.03)	(0.07)	(0.12)	(0.07)	(0.02)		

covering the photon energy range from 10 to 120 eV with two different gratings.[12] The electron-energy analyzer employed was of toroidal geometry[13] using position-sensitive detection techniques to obtain the angular information of the photoelectrons as well as their energies. All data acquired were angle resolved over the full 180° azimuth, the angular resolution being close to ±1°. The combined energy resolution of monochromator and electron analyzer was kept better than 150 meV. Measurements were performed on (110) surfaces of *n*-type-doped single crystals. To avoid charging in the case of GaP a sulfur doping of 5×10^{17} cm^{-3} was necessary due to the high electronic gap of this material of 2.27 eV.[14] The samples are prepared by cleaving *in situ* as described previously.[2] All the spectra presented here were excited with *p*-polarized light impinging under 45° along the $[1\bar{1}0]$ azimuth onto the sample because of the involved selection rules.[15]

Spectral features were identified with the help of nonlocal empirical pseudopotential (EPM) calculations. They were performed by using 113 plane waves and adjusted form factors in a Cohen-Bergstresser scheme. In order to improve the agreement between experiment and EPM calculations over the large energy range considered here it turned out to be necessary to take the nonlocal character of the pseudopotentials into account. To this end the nonlocal scheme described by Chelikowsky, Chadi, and Cohen[16] was employed in which the electron mass is allowed to vary,[17] i.e., m^* is used as an additional parameter in our EPM calculations. The form factors from Cohen and Bergstresser[18] served as a starting point for the fitting procedure. Details of the fitting procedure used for adjusting the EPM band structures to the data are described elsewhere.[2] Spin-orbit splitting is not included in these calculations. Where necessary an averaged center of gravity value for spin-orbit split-band states is used in the fitting procedure, since the splittings are expected to be smaller than the observed transition peak widths in the energy range accessible to ARCIS.

Table I lists the pseudopotential form factors obtained from fits to 16 experimentally determined symmetry point energies for GaSb and GaP (from Ref. 14 and this work, respectively). The values in parentheses, taken from Ref. 18, served as the starting point for the fitting procedure. Tables II and III give eigenvalues at the symmetry points Γ, X, and L calculated with these form factors. For simplicity the eigenvalues are denoted by symmetry point and energy-band index, e.g., the lowest-energy band at the zone center is written $\Gamma(1)$. The energy zero is taken to be the VBM.

Previous EPM calculations for conduction-band states up to 5 eV of GaP (Ref. 19) were adjusted using spectroscopic ellipsometry data only. The differences between the two sets of eigenvalues are very large. As far as we know no calculated higher conduction-band state energies for both GaP and GaSb have been reported as yet.

III. METHODOLOGICAL ASPECTS

Figure 1 shows an ARCIS spectrum of GaSb. Here the intensity distribution of the photoelectrons is shown as a function of emission angle and photon energy in a contour plot. The maximum centered at 0° corresponds to electrons photoexcited from the VBM as initial state. The highest intensity occurs for $h\nu\approx20$ eV and is confined to normal emission. By comparison, the emis-

TABLE II. Eigenvalues at points of high symmetry for GaSb. Energies are given in eV with respect to the valence-band maximum.

Band	Γ	X	L
1	−10.07	−8.06	−8.71
2	0	−5.59	−5.23
3	0	−2.01	−0.85
4	0	−2.01	−0.85
5	1.04	1.50	1.21
6	3.26	1.68	3.91
7	3.26	9.70	3.91
8	3.26	9.70	7.68
9	6.99	10.21	9.52
10	6.99	10.52	9.52
11	7.16	10.60	9.65
12	10.83	10.60	10.56
13	10.83	11.12	10.56
14	10.83	11.18	11.12
15	12.92	16.23	16.97
16	21.93	16.55	17.05
17	21.93	16.60	18.91
18	21.93	16.60	18.91
19	22.68	17.29	19.68
20	22.68	17.79	19.68
21	22.72	18.39	22.44
22	22.72	18.39	22.92
23	22.72	25.00	23.31
24	23.63	25.00	23.87
25	23.63	25.05	23.87
26	23.63	25.22	24.70
27	24.11	27.87	24.70

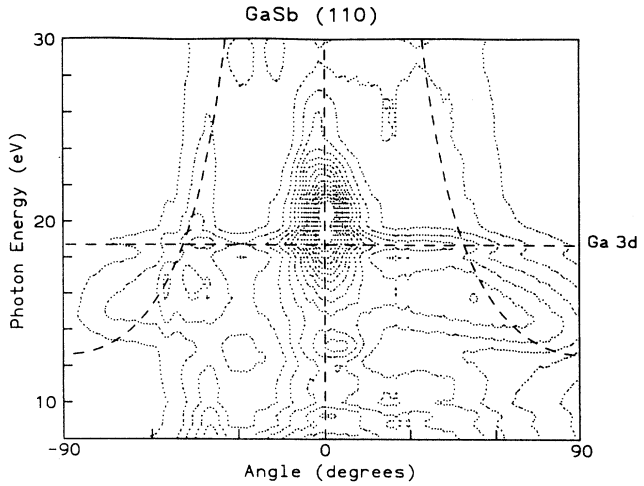

FIG. 1. Contour plot of an ARCIS spectrum of GaSb (110) in the [1$\bar{1}$0] azimuth. An interband transition manifests itself as a peak in energy and angle in contrast to the Ga 3*d* second-order core-level emission which is spread over all angles. The dashed hyperbolic lines indicate the possible locations of surface umklapp transitions.

sion at $h\nu = 18.6$ eV, due to Ga 3*d* core electrons excited by second-order light, is far more spread out in angle. Because core levels are strongly localized in real space, they are extended in **k** space and contribute therefore to the spectrum at all angles. By inspection of the angular distribution of a feature it is thus possible to distinguish direct transitions at Γ from others.

TABLE III. Eigenvalues at points of high symmetry for GaP. Energies are given in eV with respect to the valence-band maximum.

Band	Γ	X	L
1	−13.18	−10.44	−11.30
2	0	−6.88	−6.63
3	0	−2.45	−1.01
4	0	−2.45	−1.01
5	2.89	2.35	2.59
6	5.46	2.73	6.33
7	5.46	13.10	6.33
8	5.46	13.10	9.59
9	9.88	14.59	12.82
10	10.41	14.74	13.20
11	10.41	16.10	13.20
12	15.97	16.46	16.15
13	15.97	16.46	16.15
14	15.97	17.05	17.94
15	15.98	20.95	23.76
16	30.62	21.78	24.60
17	30.62	23.26	26.40
18	30.62	23.26	26.40
19	32.44	25.31	28.55
20	32.44	27.24	28.55
21	32.44	27.42	29.82
22	32.68	27.42	31.75
23	32.68	35.80	32.04
24	34.08	35.80	34.21
25	34.08	35.95	34.21
26	34.08	36.75	35.65
27	35.19	38.80	35.65

The dashed hyperbolic lines in Fig. 1 indicate the locations of possible surface umklapp transitions from the VBM at Γ. Periodicity parallel to the crystal surface implies that the component of the photoelectron momentum parallel to the surface is conserved to within a surface reciprocal lattice vector **g** so that the momentum $\mathbf{k}_{\parallel}^{\text{ext}}$ outside the crystal is given by $\mathbf{k}_{\parallel}^{\text{ext}} = \mathbf{k}_{\parallel}^{\text{int}} \pm \mathbf{g}$. Surface umklapp transitions are very weak and so there are no strong contributions to be seen in the spectra.

The proper choice of the initial state is important in an ARCIS experiment. Care must be taken with respect to occupied surface states around the VBM. In case of GaP there is an anion derived occupied band of surface states located at −0.4 eV below the VBM at $\bar{\Gamma}$, the center of the surface Brillouin zone.[8] Away from $\bar{\Gamma}$ the surface band disperses downward along the [1$\bar{1}$0] azimuth to reach −1.0 eV at $\bar{X}$. We therefore determined the VBM as described in our previous paper.[2]

The situation in GaSb is more complicated. In a detailed ARPES study of emission near the VBM Manzke *et al.*[10] determined the position of an occupied surface band state at $\bar{\Gamma}$ to lie 0.2 eV above the VBM. They fitted two peaks into a spectrum at 23 eV photon energy, regarding one as the bulk valence-band contribution and the second one as a very weak surface state (Fig. 3 in Ref. 10). Hansson and Uhrberg, however, explained Manzke's data in a different way.[20] They suggest that the supposed surface state emission originates in the topmost (heavy-hole) valence band and identify the "bulk valence-band" contribution in the 23-eV spectrum in Ref. 10 with the light-hole band. We cannot contribute to this discussion, but we find the explanation of Hansson and Uhrberg more convincing. That is why we assume the absence of an occupied surface state above the VBM and determine the VBM for GaSb as described before.[2]

In addition, surface states have an undefined $k_{\perp}$ component and their contribution to a constant-initial-state (CIS) spectrum will therefore resemble the one-dimensional density of final states along $k_{\perp}$ weighted with the appropriate matrix elements. Therefore, their contribution would in general not yield sharp intensity maxima in the CIS spectra as observed.

During the recording of the ARCIS spectra the photoemission current from the last focusing mirror in the beam line was monitored. By neglecting an energy-dependent electron yield this current is proportional to the photon flux leaving the monochromator and can thus in principle be used to normalize CIS spectra to the exciting photon flux. Despite the problems with the normalization which we discussed in the previous paper,[2] we have decided to show both raw and normalized data because in the case of GaP the peak positions are shifted noticeably by the normalization. Therefore, we present in Figs. 3(a)–3(d) the raw data as curve *a* and the normalized ones as curve *b*, respectively.

IV. RESULTS AND DISCUSSION

Figures 2(a) and 2(b) show normal emission ARCIS spectra of GaSb and GaP. Upper curves display CIS

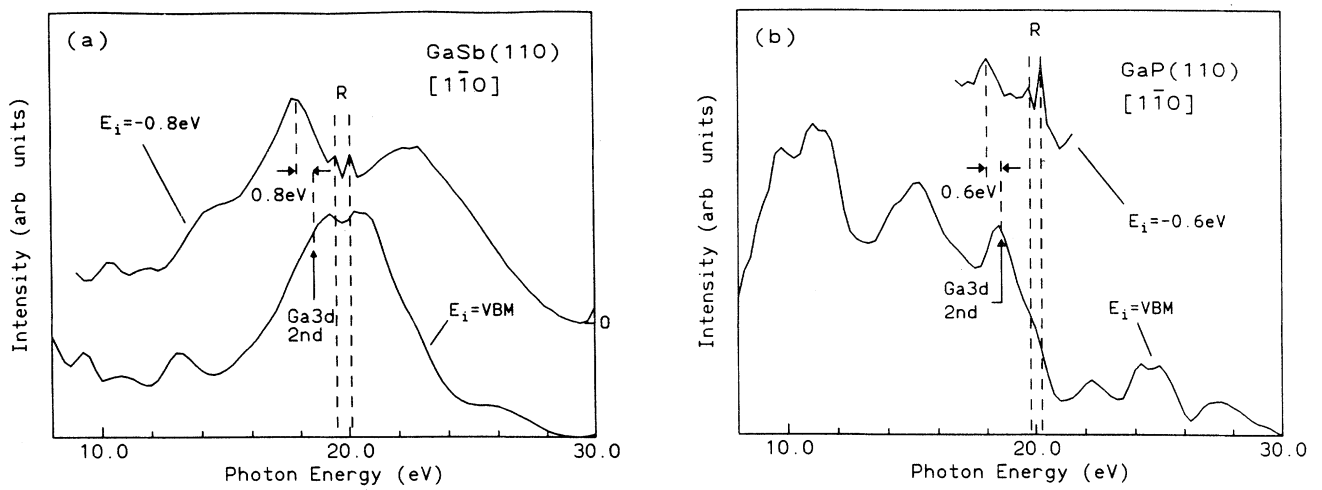

FIG. 2. Normal emission ARCIS spectra for (a) GaSb and (b) GaP in the energy range between 8 and 30 eV. The bottom curves show the spectra with the VBM as initial states while the initial-state energies of the upper curves are chosen to lie 0.8 and 0.6 eV below the VBM, respectively. Label *R* indicates surface core-exciton resonances and the second- and third-order light contributions are labeled as 2nd and 3rd, respectively.

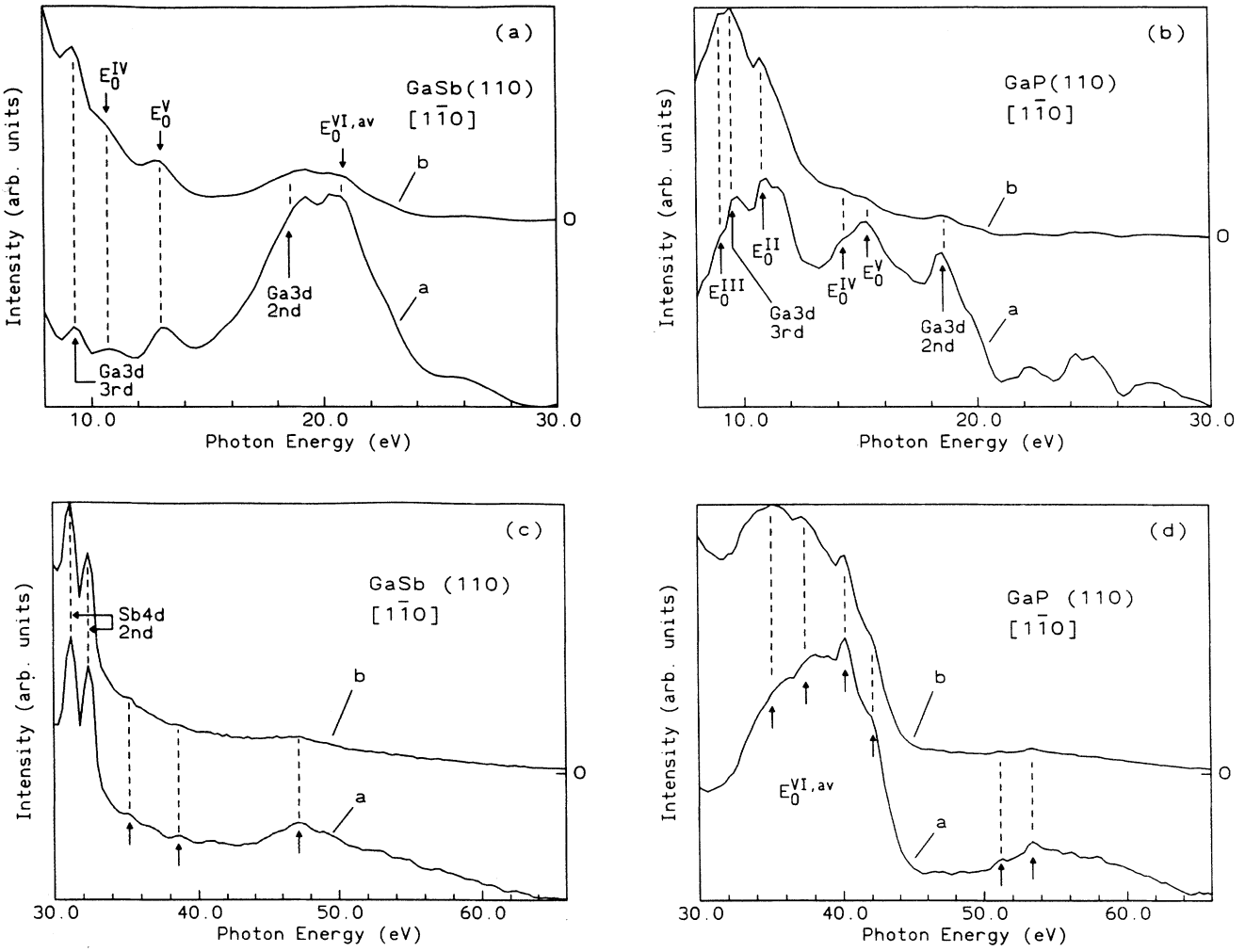

FIG. 3. Normal emission ARCIS spectra for GaSb and GaP (110) in (a) and (b) the low-energy range and (c) and (d) in the high-energy range. The bottom curve (*a*) displays the original data and the top spectrum (*b*) is normalized to the mirror current.

recorded at binding energies below the VBM. There the surface core exciton resonances labeled R are clearly identified, which will be discussed in Sec. IV A. Core levels excited by second- and third-order light give rise to the peaks identified by the core level and the labels 2nd and 3rd, respectively.

In Figs. 3(a)–3(d) normal emission ARCIS spectra of GaSb and GaP are shown for photon energies from 8 to 66 eV. In Figs. 3(a) and 3(b) the low-energy data with photon energies below 30 eV are shown while in Figs. 3(c) and 3(d) the high-energy data are presented.

Jackson and Allen determined the self-energy corrections for various semiconductor conduction-band states experimentally.[21] They estimated the lifetime broadening as a function of photoelectron energy from escape depth data. This broadening increases nearly linearly from zero up to 5 eV for final-state energies between 0 and 30 eV. Because of this we expect widths between 1 and 5 eV in the range considered in Figs. 3(a) and 3(b) and between 5 and 10 eV in the range of photon energies above 30 eV.

On account of this rather large intrinsic width of all transitions spectra were recorded in steps of 0.25 eV so that the experimental resolution is still considerably better than the expected peak widths. However, the spin-orbit splitting of the Ga 3d level [0.4 eV (Ref. 14)] is not clearly resolved with this stepwidth whereas that of the Sb 4d level [1.2 eV (Ref. 14)] is. Positions of peaks and shoulders are determined via the second derivative of the spectra after smoothing. The uncertainty in energies is 0.2 eV including errors in monochromator calibration.

A. Surface core-exciton resonances

The features labeled R in Figs. 2(a) and 2(b) are due to resonances where oscillator strength is transferred from a surface core exciton to a valence electron. This enhancement of the primary-electron yield occurs when the photon energy is sufficient to excited transitions from a core level to an empty localized surface state. The decay of this state yields the enhancement.

The surface core exciton resonances are evident in the ARCIS spectra for both materials as shown in Fig. 2 for initial-state energies below the VBM. Their energies are independent of the initial-state energies as was demonstrated in our previous paper.[2] The excitation energy of the second-order core line emission, however, depends on the initial-state energy as expected. This is apparent in Fig. 2(b) for GaP where the core line is shifted by 0.6 eV between the two spectra, i.e., by the difference in E_i.

For GaP [Fig. 2(b)] the resonance energies for excitation from the Ga $3d_{3/2}$ and $3d_{5/2}$ core levels are determined as 20.2 and 19.8 eV, respectively. They manifest themselves as very sharp peaks in the spectrum compared to the second-order core level where the spin-orbit splitting is not resolved. The binding energy of the core level's $3d_{5/2}$ component is determined as 18.6 eV in our study. Note that the intensities of the two resonances are inverted compared to the direct core-level emission which follows the statistical ratio of 2:3. This intensity conversion is particularly well documented for the In 4d levels of InP and InAs in our previous paper.[2] Such an intensity reversal has been explained by a theory[22] which takes into account the fact that the exciton oscillator strength depends strongly on the Coulomb exchange interaction between the localized states participating in this process.

In Table IV we list the binding energies of the core levels and the resonance photon energies $E_{\rm res}$. In this table previously published data are included as well.[7,23] Sette *et al.*[7] determined $E_{\rm res}$ by means of CIS and constant-final-state spectroscopy while Eastman and Freeouf[23] used photoelectron yield spectroscopy.

For GaSb [Fig. 2(a)] the autoionizing resonance is not resolved in our data at the VBM nor is the second-order core line emission. They both vanish under the strong transition labeled $E_0^{\rm VI,av}$. This peak is related to the interband transitions which will be discussed in Sec. IV B. In the CIS spectrum for $E_i=-0.8$ eV, however, both

TABLE IV. Compilation of data used to calculate the binding energies of surface core excitons. The symbols have the following meaning: $E(3d_{5/2})$, binding energy of the Ga $3d_{5/2}$ with respect to the VBM; $E_{\rm res}$, photon energy at which the surface core exciton resonance is observed; $\Delta E'=E_{\rm res}-E(3d_{5/2})$; $\Delta E=E_{\rm res}-[E(3d_{5/2})+\delta_{SC}]$ where $\Delta_{SC}=0.3$ eV corresponds to the surface core level shift; $E_{\rm exc}$, core exciton binding energy calculated with the average ΔE and the position of the lowest empty surface state at $\bar{X}$.

	Ref.	Cation core level $E(3d_{5/2})$ (eV)	Resonance $E_{\rm res}$ (eV)	$\Delta E'$ (eV)	ΔE (eV)	Surface band states (eV)		$E_{\rm exc}$ (eV)
GaSb	a	18.7	19.5	0.8		1.9($\bar{\Gamma}$)	d	
	b	18.7	19.3	0.6		1.0($\bar{X}$)	d	0.6
	av	18.7	19.4±0.1	0.7±0.1	0.4±0.1			
GaP	a	18.6	19.8	1.2		3.0($\bar{\Gamma}$)	e	
	c	18.4	19.8	1.4		2.4($\bar{X}$)	e	1.4
	b	18.4	19.6	1.2				
	av	18.5±0.1	19.7±0.1	1.3±0.1	1.0±0.1			

[a]This work.
[b]Reference 23.
[c]Reference 7.
[d]Reference 5.
[e]Reference 4.

features are resolvable. There we determine Ga $3d_{3/2}$ and $3d_{5/2}$ resonance energies of 20.1 and 19.5 eV, respectively. These values are listed together with the data of Ref. 23 and the core-level binding energy in Table IV.

The quantity of interest is the core-exciton binding energy E_{exc}. This is the difference between the exciton energy and the one-electron energy difference of the two levels involved. Therefore it is necessary to know the energy of the empty surface state band exactly. Because this quantity is not readily available the difference $\Delta E'$ between the exciton excitation energy and the core-level binding energy with respect to the VBM is usually quoted (see Table IV).

For the further analysis we use averages of the experimental entries in Table IV. For both GaP and GaSb it is necessary to include a surface chemical shift in the core-level binding energies for further evaluations because the surface core exciton is confined to the surface region. For both materials the cation level was found to be shifted by 0.3 eV towards higher binding energies in atoms of the first atomic layer.[24,25] The surface core electrons are more strongly bound than bulk core electrons. This surface shift is included in the values for ΔE of Table IV.

For the determination of the binding energy of the surface core exciton the position of the lowest surface conduction band is required. GaP has long been considered an exception among III-V compounds as far as the energy of this band is concerned. Previous KRIPES measurements located this band at 1.96 or 0.3 eV below the bulk conduction-band minimum.[26] A more recent study by Perfetti and Reihl,[4] however, places it at 3.0 eV at $\bar{\Gamma}$ and at 2.4 eV at $\bar{X}$ with respect to the VBM, respectively. This means a position well above the bulk conduction-band minimum. The latter values for $\bar{\Gamma}$ and $\bar{X}$ are also listed in Table IV. Inverse photoemission data for GaSb (Ref. 5) are quoted as well.

We thus calculate an exciton binding energy with respect to the surface conduction-band minimum of 0.6 eV for GaSb and of 1.4 eV for GaP. These energies are comparable to 0.8 eV for GaAs, 1.2 eV for InP, and 0.5 eV for InAs, respectively, which were determined in our previous work.[2] They are also in reasonable agreement with theoretical estimates that yield a binding energy of 1.07 eV.[27]

B. Interband transitions

We now proceed to the discussion of the band transitions and return to the spectra of Fig. 3. All structures which are not yet identified as core-level emissions or resonances are possible candidates for interband transitions at the center of the Brillouin zone.

The assignment of the spectral features to particular band transitions was achieved by comparison with our EPM calculations. The labeling of the transitions follows the one introduced in the optical literature where E_0 stands for electronic gap at Γ. Transitions E_0^{II} and E_0^{III} in GaP, E_0^{IV}, E_0^{V}, and $E_0^{VI,av}$ for both materials are identified here.

In a first approach we consider transitions from the VBM into FEP final states. Assuming an inner potential of 9.0 eV for both materials we expect transitions to the (200) umklapp regime at 7.2 eV for GaSb and 11.3 eV for GaP and to the (220) umklapp at 23.4 and 31.5 eV, respectively. Transitions labeled E_0^{II} and $E_0^{VI,av}$ are close to the predicted values. We will discuss the relation between the experimental transitions and the FEP later where we assign particular transitions to different umklapps of the FEP.

Considering the peaks around 21 eV in GaSb and around 35 eV in GaP first, we assign them to states derived from the (220) umklapp of the FEP. These transitions are expected to be strongest in spectra taken in normal emission on (110) surfaces.[28] Transitions into the (220) branch of the FEP's couple particularly well to the outgoing wave along the normal [110] direction ("primary cone emission"). This explains their high intensity in the spectra shown in Fig. 3.

On the basis of the correspondence between EPM and experimental energies transitions have been assigned to specific final states as listed in Table V. The labeling follows the one introduced in the optical literature with respect to the representations. The energetic order of the transitions E_0^i can change between different materials because of differences in the details of the band structures. The EPM conduction-band energies are listed in Table II for GaSb and in Table III for GaP, respectively. Peaks are identified up to $E_0^{VI,av}$, which denotes the group of transitions derived from the (220) umklapp of the FEP. However, we are in no position to assign structure in the (220) umklapp region of the spectra to particular band transitions due to the large number of final states in close vicinity. We therefore label this group $E_0^{VI,av}$ and list the center of gravity in Table V for this transition only.

To our knowledge no work has been done concerning bulk conduction-band states in this energy range for both materials. Therefore we compare the results for GaSb and GaP with our previous data for GaAs, InP, and InAs.[2] The band structures of the III-V compounds considered here are very similar despite the fact that GaP is an indirect semiconductor whereas all other compounds are direct. Due to the small lattice constant of 5.45 Å in GaP all energies are shifted to higher values compared to GaSb with a lattice constant of 6.10 Å. A major difference is that in the case of GaP the E_0^{III} transition is

TABLE V. Interband transitions at Γ as determined in this work. Energy values for transitions below 8 eV are taken from the literature. $E_0^{VI,av}$ designates the center of gravity of a number of transitions derived from the (220) umklapp.

	$\Gamma_{15}^{v}\rightarrow$	GaSb	GaP
E_0	Γ_1^c	0.81[a]	2.78[a]
E_0'	Γ_{15}^c	3.19[a]	4.87[a]
E_0^{II}	Γ_{12}^c	7.9[a]	10.8
E_0^{III}	Γ_1^c		9.0
E_0^{IV}	Γ_{15}^c	10.7	14.3
E_0^{V}	Γ_1^c	13.0	15.2
$E_0^{VI,av}$	$\Gamma_?^c$	20.8	37.6

[a]Reference 14.

strong and thus resolvable in our spectrum. In all the other materials this transition has not been detected by means of ARCIS. This agrees with our intensity calculations where we obtain a ratio of 1:3 for the intensities of E_0^{III}:E_0^{II} in GaP, whereas for all the other materials this ratio is 1:10 or less.

In the process of adjusting the EPM calculations to the experimental transition energies the effective electron mass m^* was allowed to vary as mentioned before and typically turned out to be slightly larger than one. For GaP, however, we inevitably obtained a value less than one. By disregarding the $E_0^{VI,av}$ transition group in the fitting procedure, however, the value of m^* turned out to be larger than one as well. This behavior is reasonable because the $E_0^{VI,av}$ group for GaP is about 6 eV higher in energy than the comparable FEP state.

By closer inspection of the symmetry of the final states for the E_0^i transitions (i=I,II,...) theory origin in the free-electron parabola can be found. The symmetries of the free-electron final-state Γ points are quoted in a recent paper by Niles, Rioux, and Höchst.[29] By turning on the crystal potential the symmetries of the free-electron states remain unchanged while the degeneracy is lifted. In the following, these nondegenerate states are denoted in the standard notation of the corresponding representation.[30]

The origin of the free-electron parabola is nondegenerate, the (111) umklapp is fourfold, the (200) umklapp is threefold, and the (220) umklapp is fivefold degenerate. The irreducible representation of the origin of the parabola has Γ_1 symmetry and the (111) umklapp is associated with two Γ_1 and two Γ_{15} representations for example. By turning on the crystal potential Γ_1^v as the valence-band minimum, Γ_{15}^v as its maximum, and two Γ_1^c and one Γ_{15}^c in the conduction band are derived from these free-electron states. By comparing the band transitions E_0^i in Table V with these final-state symmetries it is obvious that the final states of the E_0, the E_0^I, and the E_0^{III} transitions originate in the (111) umklapp of the free-electron parabola.

Following this method, the (200) umklapp splits into the final states of the E_0^{II}, the E_0^{IV}, and the E_0^V transition. In the same manner $E_0^{VI,av}$ has its origin in the (220) umklapp of the free-electron model. This explains the strong intensity found for the $E_0^{VI,av}$ transition in the [110] direction. In summary, it is thus possible to assign particular band transitions to FEP umklapp energies.

Figure 4 shows a comparison of the band transitions for GaSb, InAs, InP, GaAs, and GaP. There the transition energies are plotted versus G_{220}, the smallest reciprocal lattice vector in the [110] direction. The dashed lines indicate the position of the (111), (200), and (220) umklapps of the FEP, respectively. For its calculation we used an average inner potential of 9.0 eV, as mentioned above. Squares indicate transitions that are derived from the (220) umklapp, diamonds from the (200) umklapp, and crosses from the (111) umklapp, respectively. The data presented here are taken from Table V and from Table VII of our previous paper.[2] Energy values above 8.5 eV are determined by us while the lower-energy data are taken from the literature.[14]

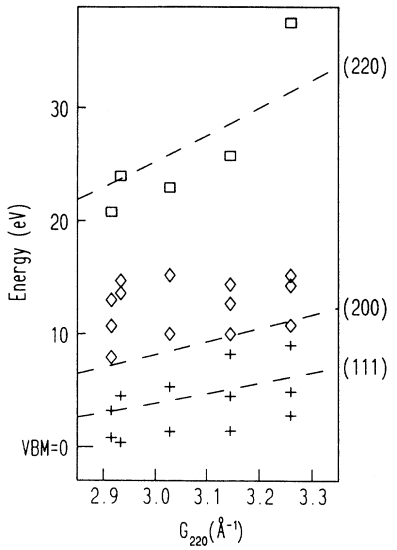

FIG. 4. Comparison of interband transition energies for the different materials. The energies are plotted vs the length of the reciprocal lattice vector G_{220}. The meaning of the different symbols is explained in the text.

Deviations between the FEP and the experimental results are observed. See, for example, the deviations of the transitions derived from the (200) umklapp and the FEP energies. A systematic tendency with the lattice constant cannot be established in general. The FEP model thus appears to work well within the Brillouin zone as demonstrated by ARPES work, but not at points of high symmetry such as, for example, Γ or X. Note that for the calculation of the FEP energies an inner potential of 9.0 eV was taken for all the materials justified by our previous work, whereas potentials of 6.92 eV for GaSb (Ref. 11) and of 9.5 eV for GaP (Ref. 8) have been reported by other authors.

Above the feature $E_0^{VI,av}$ an assignment of structure in the CIS spectra to particular final states is impossible. According to our transition probability calculations allowed transitions in this energy range are expected to be very weak. The strongest transition in the high-energy region in case of GaSb is the second-order core-level emission from the Sb 4d level. Additional structures are seen at 35.1, 38.6, and 47.2 eV. The latter transition is the most intense one. For GaP there is structure at 51.2 and 53.4 eV. A correspondence between the two sets of transitions could not be established.

V. CONCLUSION

Angle-resolved constant-initial-state spectra have been performed to study conduction-band critical points at the center of the Brillouin zone up to 66 eV above the VBM in GaSb and GaP. Experimental features below 40 eV have been identified with direct interband transitions on the basis of EPM calculations with optimized pseudopotential form factors. A correspondence between the free-electron model and the identified band transitions was investigated. The data were also compared with our previ-

ous measurements on GaAs, InP, and InAs. All the systems exhibit similar transitions aside from the E_0^{III} transition which was only identified in GaP. However, a systematic trend with the lattice constant expected on the basis of the free-electron model could not be established in general.

Above about 40 eV a number of structures are observed experimentally that also do not exhibit trends in energy as expected for interband transitions on the basis of different lattice constants. There structures cannot be explained in terms of either the free-electron model or an EPM calculation even if an element of nonlocality is introduced in the latter through the adjustment of the effective electron mass. The origin of these structures must therefore be sought outside the scope of simple interband transitions or more sophisticated band structure calculations are needed for their explanation.

Finally, autoionization resonances involving surface core excitons have been observed in both materials. From these an estimate of the surface core-exciton binding energy could be derived that compares favorably with pertinent calculations.

ACKNOWLEDGMENTS

This work was supported by the Bundesministerium für Forschung und Technologie, Contract No. 055 WEDA B 3, and by the Australian Research Council. The authors would like to thank the staff of BESSY for their help and hospitality during the experiments. Thanks are also due to the Institut für Werkstoffwissenschaften VI in Erlangen, especially to G. Müller, F. Mosel, G. Neuner, and Ch. Weber for cutting and orientating the GaP crystals. We also acknowledge the assistance of R. Denecke, T. Seyller, J. Con Foo, and C. Russel during the experiments.

*Present address: Fritz-Haber-Institut, Faradayweg 4-6, D-14195 Berlin, Germany.

[1]R. C. G. Leckey and J. D. Riley, Crit. Rev. Solid State Mater. Sci. **17**, 307 (1992).
[2]J. Faul, G. Neuhold, L. Ley, J. Fraxedas, S. Zollner, J. D. Riley, and R. C. G. Leckey, Phys. Rev. B **47**, 12 625 (1993).
[3]W. Drube, D. Straub, and F. J. Himpsel, Phys. Rev. B **35**, 5563 (1987).
[4]P. Perfetti and B. Reihl, Phys. Scr. **T25**, 173 (1989).
[5]R. Manzke and M. Skibowski, Phys. Scr. **T31**, 87 (1990).
[6]J. A. Knapp and G. J. Lapeyre, Nuovo Cimento B **39**, 693 (1977).
[7]F. Sette, P. Perfetti, F. Patella, C. Quaresima, C. Capasso, M. Capozi, and A. Savoia, Phys. Rev. B **28**, 4882 (1983).
[8]F. Solal, G. Jezequel, F. Houzay, A. Barski, and R. Pinchaux, Solid State Commun. **52**, 37 (1984).
[9]G. P. Williams, F. Cerrina, G. J. Lapeyre, J. R. Anderson, R. J. Smith, and J. Hermanson, Phys. Rev. B **34**, 5548 (1986).
[10]R. Manzke, H. P. Barnscheidt, C. Janowitz, and M. Skibowski, Phys. Rev. Lett. **58**, 610 (1987).
[11]T. C. Chiang and D. E. Eastman, Phys. Rev. B **22**, 2940 (1980).
[12]W. Braun and G. Jäkisch, Ann. Israel Phys. Soc. **6**, 30 (1983).
[13]R. C. G. Leckey and J. D. Riley, Appl. Surf. Sci. **22/23**, 196 (1985).
[14]*Numerical Data and Functional Relationships in Science and Technology,* Landolt-Börnstein, New Series III/22a and 23a (Springer-Verlag, Berlin, 1989), and references therein.
[15]J. Hermanson, Solid State Commun. **22**, 9 (1977).
[16]J. Chelikowsky, D. J. Chadi, and M. L. Cohen, Phys. Rev. B **8**, 2786 (1973).
[17]R. A. Pollak, L. Ley, S. Kowalczyk, D. A. Shirley, J. D. Joannopoulos, D. J. Chadi, and M. L. Cohen, Phys. Rev. Lett. **29**, 1103 (1972).
[18]M. L. Cohen and T. K. Bergstresser, Phys. Rev. **141**, 789 (1966).
[19]S. Zollner, M. Garriga, J. Kircher, J. Humliček, M. Cardona, and G. Neuhold, Thin Solid Films (to be published); Phys. Rev. B **48**, 7915 (1993).
[20]G. V. Hansson and R. I. G. Uhrberg, Surf. Sci. Rep. **9**, 197 (1988).
[21]W. B. Jackson and J. W. Allen, Phys. Rev. B **37**, 4618 (1988).
[22]Y. Onodera and Y. Toyozawa, J. Phys. Soc. Jpn. **22**, 833 (1967).
[23]D. E. Eastman and J. L. Freeouf, Phys. Rev. Lett. **34**, 1624 (1975).
[24]A. B. McLean and R. Ludeke, Phys. Rev. B **39**, 6223 (1989).
[25]V. Hinkel, L. Sorba, and K. Horn, Surf. Sci. **194**, 597 (1988).
[26]D. Straub, M. Skibowski, and F. J. Himpsel, J. Vac. Sci. Technol. A **3**, 1484 (1985).
[27]R. Del Sole and E. Tosatti, Solid State Commun. **22**, 307 (1977).
[28]G. D. Mahan, Phys. Rev. B **2**, 4334 (1970).
[29]D. W. Niles, D. Rioux, and H. Höchst, Phys. Rev. B **46**, 12 547 (1992).
[30]L. P. Bouckaert, R. Smoluchowski, and E. Wigner, Phys. Rev. **50**, 58 (1936).